mathematics

MDPI

Article

Modelling Soil Compaction Parameters Using an Enhanced Hybrid Intelligence Paradigm of ANFIS and Improved Grey Wolf Optimiser

Abidhan Bardhan [1], Raushan Kumar Singh [2], Sufyan Ghani [3], Gerasimos Konstantakatos [4] and Panagiotis G. Asteris [4,*]

[1] Department of Civil Engineering, National Institute of Technology, Patna 800005, India; abidhan@nitp.ac.in
[2] Department of Computer Engineering and Applications, GLA University, Mathura 281406, India; raushan.singh@gla.ac.in
[3] Department of Civil Engineering, Sharda University, Greater Noida 201310, India; sufyan.ghani@sharda.ac.in
[4] Computational Mechanics Laboratory, School of Pedagogical and Technological Education, 14121 Athens, Greece; gkonstantakatos@aspete.gr
* Correspondence: asteris@aspete.gr

Abstract: The criteria for measuring soil compaction parameters, such as optimum moisture content and maximum dry density, play an important role in construction projects. On construction sites, base/sub-base soils are compacted at the optimal moisture content to achieve the desirable level of compaction, generally between 95% and 98% of the maximum dry density. The present technique of determining compaction parameters in the laboratory is a time-consuming task. This study proposes an improved hybrid intelligence paradigm as an alternative tool to the laboratory method for estimating the optimum moisture content and maximum dry density of soils. For this purpose, an advanced version of the grey wolf optimiser (GWO) called improved GWO (IGWO) was integrated with an adaptive neuro-fuzzy inference system (ANFIS), which resulted in a high-performance hybrid model named ANFIS-IGWO. Overall, the results indicate that the proposed ANFIS-IGWO model achieved the most precise prediction of the optimum moisture content (degree of correlation = 0.9203 and root mean square error = 0.0635) and maximum dry density (degree of correlation = 0.9050 and root mean square error = 0.0709) of soils. The outcomes of the suggested model are noticeably superior to those attained by other hybrid ANFIS models, which are built with standard GWO, Moth-flame optimisation, slime mould algorithm, and marine predators algorithm. The results indicate that geotechnical engineers can benefit from the newly developed ANFIS-IGWO model during the design stage of civil engineering projects. The developed MATLAB models are also included for determining soil compaction parameters.

Keywords: soil compaction; adaptive neuro-fuzzy inference system; grey wolf optimiser; swarm intelligence

MSC: 68Txx

Citation: Bardhan, A.; Singh, R.K.; Ghani, S.; Konstantakatos, G.; Asteris, P.G. Modelling Soil Compaction Parameters Using an Enhanced Hybrid Intelligence Paradigm of ANFIS and Improved Grey Wolf Optimiser. *Mathematics* **2023**, *11*, 3064. https://doi.org/10.3390/math11143064

Academic Editor: Gaige Wang

Received: 23 June 2023
Revised: 6 July 2023
Accepted: 7 July 2023
Published: 11 July 2023

1. Introduction

In the parlance of geotechnical engineering, soil compaction is a method of compressing soil particles by reducing air voids while maintaining steady water content [1,2]. Compaction can be used to enhance the mechanical qualities of soils in a number of different ways. Proctor [3] recommended compacting soil with different water contents at an appropriate compaction energy. As a result, the compaction curve can be used to determine the optimum moisture content (OMC) and maximum dry density (MDD) of soils. To sustain the long-term performance of various engineering structures, such as embankments of railways, highways, and airport runways, these two compaction parameters are commonly

used [4–8]. Understanding and predicting the compaction characteristics of different soils is thus a crucial aspect of every construction project [9–13].

Analytical techniques and laboratory experiments can be used to calculate the OMC and MDD [1,14,15]. However, to precisely characterise the compaction curve, at least 4 to 5 tests must be carried out in the laboratory, which takes a long time [9,14]. In order to conduct tests and obtain accurate results, highly qualified technical staff and expert personnel are needed. The laboratory values of OMC and MDD are utilised to compact soils of sub-base/base layers to achieve 95–98% MDD in the field. Thus, it is important to create smart, data-driven algorithms for calculating the OMC and MDD based on existing experimental records [1,15,16]. To determine the OMC and MDD of soils, a number of prediction models have previously been put forth. Regression analysis and different data from particular soils were used to create the majority of these models. However, according to the literature, the prediction accuracy of these models tends to decrease as the size of the database increased [1,14,17].

In order to address the issue with a larger database and improved accuracy, machine learning techniques (MLTs) have recently been employed to estimate the OMC and MDD of soils. Using evolutionary polynomial regression (EPR) and artificial neural networks (ANNs), the compaction characteristics of 55 soil samples were predicted [18]. The group method of data handling (GMDH) was used by Ardakani and Kordnaeij [19] to estimate the compaction parameters of 212 samples. Based on the results of 451 experiments using the index properties and conventional proctor tests, Kurnaz and Kaya [16] employed GMDH, support vector machine (SVM), extreme learning machine (ELM), and Bayesian regularisation neural network to estimate the OMC and MDD of soils. Recently, Tiwari et al. [17] used hybrid least square support vector machine (LSSVM) approaches to estimate the OMC and MDD of soils, and found satisfactory results.

These prediction models, in comparison to regression analysis models, displayed better determination coefficient (R^2) values, ranging from 0.90 to 0.98 [1,14]. Nevertheless, these studies used only a few different types of soils. Past studies have shown that within a given soil range, forecast accuracy can be ensured; nevertheless, the issue of the limited soil type and the inadequate consideration of soil factors may result in inaccurate predictions. Prediction models constructed and validated with the fewest number of influential parameters, which are typically determined when samples are brought to the laboratory, are also regarded as the most effective. In contrast, the nonlinear stress-strain relationships, the stress-strain time-conditioning response, and the elasto-plastic behaviour under loading and unloading conditions make soil materials highly complex [20–24]. Therefore, a high-performance soft computing model is considered necessary to estimate the OMC and MDD of soils, taking into account a wide range of soil types and the most influential variables (such as grain size analysis, plasticity characteristics, etc.) that can be readily measured in the laboratory.

According to the most recent literature, ensemble-based and hybrid MLTs are the best suited approaches for estimating the anticipated outputs, such as load-carrying capacity assessment of semi-rigid steel structures [25], patch load resistance of stiffened plate girders [26], soil compaction parameters [27], compression index [24], etc. Additionally, due to the complexity of the task at hand, it is required to look at a variety of advanced MLTs in order to find more precise estimating models. A detailed review of the literature reveals that the main advantage of the neuro-fuzzy system is that it combines neural network properties with fuzzy logic; hence, eliminating the limitations of these two MLTs can be found in the literature [28,29]. After ANN, Adaptive neuro-fuzzy inference system (ANFIS) is one of the widely used MLTs and can be implemented easily to estimate the desired output(s). ANFIS has the advantage of knowing both numbers and languages. ANFIS also makes use of ANN's capacity to classify data and recognise patterns. Specifically, ANFIS is more transparent to the user than the ANN model and generates fewer memorisation errors. The fundamental advantage of the neuro-fuzzy system is that it blends neural network properties with fuzzy logic, removing the limitations of both. While fuzzy logic

deals with knowledge that can be obtained and comprehended, neural networks deal with knowledge that can be obtained only via optimised learning [28,30]. However, like many other MLTs, ANFIS has some limitations, such as overfitting issues. Additionally, because it is hard to define the exact global optimum, it may produce undesirable outcomes during the validation phase [14,31].

To solve these issues, researchers have employed a number of meta-heuristic algorithms (MHAs), such as GA, PSO, GWO, etc. [28,29,32], and a number of hybrid models of traditional MLTs and MHAs were built for the estimation of desired output(s). It is important to note that construction of an effective ANFIS model requires optimum selection of its consequent and antecedent (C&A) and fuzzy inference system (FIS) parameters. These two parameters significantly affect how the learning phase turns out, which in turn affects how well a hybrid ANFIS model can predict the desired variables. Due to the robust global search capabilities of MHAs, the C&A parameters of ANFIS are iteratively adjusted, resulting in improved performance. Over the past decade, several hybrid ANFIS models have seen widespread use in addressing a wide range of engineering problems, including compressive strength estimation [28,33], flood assessment [34], prophecy of groundwater level [35], and so on.

Nevertheless, a detailed review of the literature reveals that no previous study has employed hybrid ANFIS models constructed with a specific group of MHAs to predict soil compaction parameters. On the other hand, it is important to highlight that no algorithm provides perfect solutions for all optimisation problems due to improper exploration and exploitation (E&E) processes [31,36]. Therefore, implementing a standard version of MHA in hybrid modelling does not ensure optimum hybrid model generation. It may also be noted that researchers reported modified versions of MHAs and demonstrated that the performance of standard MHA could be improved by implementing different strategies [37–39]. Considering these points as a reference, and to fill the gap in the literature, an enhanced hybrid technique of ANFIS and an improved grey wolf optimiser (IGWO), i.e., ANFIS-IGWO, has been constructed and presented in this study for the estimation of OMC and MDD of soils. The performance of the ANFIS-IGWO model was compared to that of three hybrid ANFIS models built using moth-flame optimisation (MFO), slime mould algorithm (SMA), and marine predator algorithm (MPA). The performance of the ANFIS-IGWO model was also compared with the standard hybrid model of ANFIS and GWO, i.e., ANGIS-GWO. Thus, as a part of ongoing research and to extend the work of Bardhan and Asteris [14], a suitable database of various soils was compiled from the studies of Günaydın [15], Wang and Yin [1], and Bardhan and Asteris [14] and a modified database was prepared. Specifically, a total of 251 datasets from 15 different soils were acquired and utilised in the current study for the estimation of the OMC and MDD of soils.

The remainder of this work is organised as follows. The significance of the present study is presented in Section 2. Section 3 details the methodological development of ANFIS-based hybrid models. Section 4 discusses data collection, descriptive details, and the computer modelling procedure. Section 5 provides and discusses the realisations of the developed models, followed by Section 6 with the limitations and future scope of the study. At the end, summary and conclusions are presented.

2. Research Significance

In the last two decades, a multitude of modern computational methods, techniques, and algorithms have been proposed and published with the aim of predicting the response of complex phenomena whose strongly non-linear nature and behaviour make impossible the widely accepted use of deterministic techniques [25,26]. In these methods, artificial intelligence, machine learning, and MHAs have a dominant position. In fact, despite the fact that these techniques started with the first applications in medicine [40], they were particularly applied in the fields of sciences [30,41–43] and engineering [44–48]. The use of contemporary intelligence techniques in geotechnical and geological engineering domains, such as landslide susceptibility mapping [49], reliability analysis [50], and es-

timation of various geotechnical parameters [24,27] can also be found in the literature. However, the existing literature in the geotechnical engineering area does not demonstrate sufficient implementation of enhanced/improved versions of MHAs in estimating various geotechnical parameters. Taking the above discussion as a reference, this study proposes a high-performance intelligence paradigm built using an upgraded version of MHA for estimating the OMC and MDD of soils.

3. Methodology

This section presented the theoretical details of GWO and IGWO, followed by a short discussion on MFO, SMA, and MPA. Subsequently, the methodological development of hybrid ANFIS models is presented and discussed. However, before presenting the above details, the working principles of the ANFIS are briefly presented.

3.1. Adaptive Neuro-Fuzzy Inference System

ANFIS, proposed by Jang [51], is an ANN-FIS integration, which was intended to eliminate the drawbacks of the individual ANN and FIS approaches. ANFIS is grounded in fuzzy logic and rules produced in the particular training procedure of the model. These inference systems contain five layers (see Figure 1). The nodes of layer 0 are the inputs, while the nodes of layer 5 represent the output in the connection-based structure. The fixed adaptable nodes of the hidden layers stand for the membership functions (MFs).

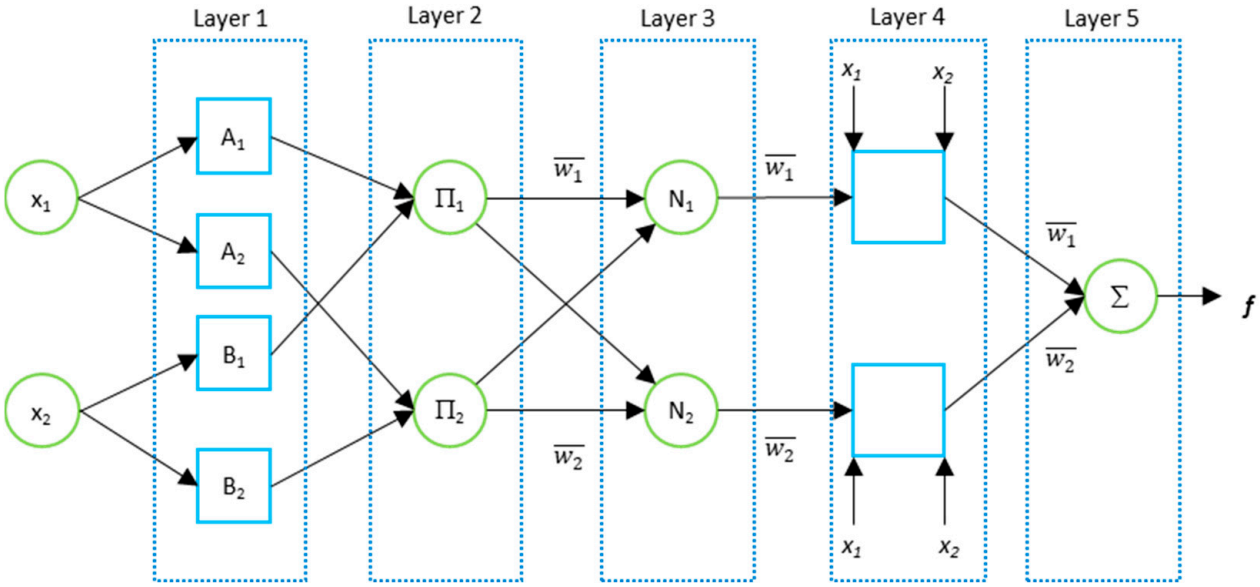

Figure 1. A basic architecture of ANFIS.

For a summarised description of the ANFIS approach, let x_1 and x_2 be the inputs. Additionally, let f be the output. The ANFIS represents the relationship between the inputs and output by fuzzy *if–then* rules. The Takagi–Sugeno fuzzy rules in the model are shown as:

Rule-1: $if\ x_1\ is\ A_1$ and $x_2\ is\ B_1$, then $f_1 = p_1x_1 + q_1x_2 + r_1$
Rule-2: $if\ x_1\ is\ A_2$ and $x_2\ is\ B_2$, then $f_2 = p_2x_1 + q_2x_2 + r_2$

where A_1, A_2, B_1, and B_2 are linguistic symbols, while p_1, q_1, r_1, p_2, q_2, and r_2 are the consequent variables. The layers include:

Layer 1: Fuzzification layer—it is assumed that node i has an adaptive function as: $O_{1,i} = \mu_{A_i}(x)$, where $O_{1,i}$ is the output of node i, while μ_{A_i} denotes the MF.
Layer 2: Ruler layer—Node i within this layer is assumed to be fixed (II). In addition, the node output is generated by incoming signals, such as $O_{2,i} = w_i = \mu_{A_i}(x) \times \mu_{B_i}(x)\ for\ i = 1, 2,$

where $O_{2,i}$ denotes the output of the second layer, and w_i represents the firing strength of rule i.
Layer 3: Normalisation layer—Node i undergoes normalisation in the third layer (firing strengths). The ratio of the firing force of rule i to the total firing force can be obtained as: $O_{3,i} = \overline{w}_i = w_i/(w_1 + w_2)$, where $O_{3,i}$ is the output of the third layer, and $\overline{w}_i$ stands for the normalised firing strength.
Layer 4: Defuzzification layer—In this layer, each of the nodes is adaptive and has a function representing the contribution of rule i to the total output.
Layer 5: Output layer—Eventually, this layer yields the final output.

ANFIS can be equipped for MF parameter identification through hybrid learning approaches. Such approaches define the parameters of the defuzzification layer using the forward least squares technique. Errors undergo backpropagation to modify a_i, b_i, and c_i as the premise parameters through gradient descent. For more details, the works of Paryani et al. [49], Piro et al. [30], Golafshani et al. [28], can be referred to.

3.2. Grey Wolf Optimiser

GWO [52] is comes under the category of evolutionary algorithm developed for optimisation based on the imitation of the grey wolves' social behaviour. Specifically, this algorithm mimics the process that grey wolves utilise to capture their prey, along with the structure of their leadership. For the recreation of the hierarchical structure in GWO, grey wolves of four different types are assumed for every wolf pack. The leader and the most significant wolf in the pack are called α, β and δ wolves. ω wolves with minimum responsibility are placed at the bottom of the food. In GWO, the entire hunting process can be classified as searching, encircling, hunting, and attacking. The mathematical expression for encircling prey is given by:

$$D = \left| C.X_{p(t)} - X_{(t)} \right| \tag{1}$$

$$X_{(t+1)} = X_{p(t)} - A.D \tag{2}$$

where X and X_p are the position vectors of the grey wolf and the prey, respectively; t and $t+1$ represent current and subsequent epochs, respectively. A and C are two vectors given by:

$$A = 2a.r_1 - a \tag{3}$$

$$C = 2.r_2 \tag{4}$$

where r_1 and r_2 are the two random vectors that are uniformly distributed [0 1], and the components of a are linearly decreased from 2 to 0. When $|A| > 1$, the exploration of prey location is possible by diverting the search agents. Conversely, with $|A| < 1$, convergence of search agents can be used to achieve exploitation. The hunting process in GWO can be mathematically modelled as follows:

$$D_\alpha = |C_1.X_\alpha - X|;\ D_\beta = \left|C_2.X_\beta - X\right|;\ D_\delta = |C_3.X_\delta - X| \tag{5}$$

$$X_{i1} = X_\alpha - A_1.(D_\alpha)\ ;\ X_{i2} = X_\beta - A_2.\left(D_\beta\right)\ ;\ X_{i3} = X_\delta - A_3.(D_\delta) \tag{6}$$

$$X_{(t+1)} = (X_{i1} + X_{i2} + X_{i3})/3 \tag{7}$$

In GWO, E&E is handled using parameters a and C, in which the parameter a is decreased from 2 to 0. Additionally, it is seen that the final position would be in a random place within a circle, which is defined by the positions of α, β, and δ in the search space. More mathematical details can be found in the original work of Mirjalili et al. [52].

3.3. Improved Grey Wolf Optimiser

In GWO, α, β, and δ guide ω wolves toward regions of the search space where the optimal solution is likely to be located. This approach may result in entanglement in a locally optimal solution. Another drawback is the decline in population diversity, which causes GWO to approach the local optimum. Nadimi-Shahraki et al. [53] proposed IGWO to address these problems. According to the study of Nadimi-Shahraki et al. [53], the enhancements involve a new search strategy involving a step of selecting and upgrading. Therefore, IGWO consists of three phases, as discussed below.

Initialising phase: During the initialisation phase, N wolves are randomly distributed in $[l_j, u_j]$, as:

$$X_{ij} = l_j + rand_j[0,1] \times (u_j - l_j),\ i \in [1,N], j \in [1,D] \quad (8)$$

The position of the i-th wolf in the t-th iteration, represented by $X_i(t) = \{x_{i1}, x_{i2}, \ldots, x_{iD}\}$, where D is the dimension number. The fitness value of $X_i(t)$ is calculated using f $(X_i(t))$.

Movement phase: The IGWO, proposed by Nadimi-Shahraki et al. [53], includes a different mobility tactic known as the dimension learning-based hunting (DLH) method, in which each wolf is learned by its neighbours to be a different contender for the new position, $X_i(t)$.

Selecting and updating phase: During this stage, the best candidate is first chosen by contrasting the fitness ratings between two candidates $X_{i\text{-}GWO}(t+1)$ and $X_{i\text{-}DLH}(t+1)$, given by:

$$X_i(t+1) = \begin{cases} X_{i-GWO}(t+1), & if\ f(X_{i-GWO}) < f(X_{i-DLH}) \\ X_{i-DLH}(t+1) & \text{otherwise} \end{cases} \quad (9)$$

Then, to update the position of $X_i(t+1)$, if the fitness of the selected candidate is less than $X_i(t)$, $X_i(t)$ is updated by the selected candidate. Otherwise, $X_i(t)$ remains unchanged. After this procedure, the iteration count is increased by 1, and the search operation is repeated until the predetermined number of epochs has been reached.

3.4. Brief Overview of MFO, SMA, and MPA

The other employed MHAs, viz., MFO, SMA, and MPA, are briefly discussed in this sub-section. All of these MHAs are swarm-based and they have been widely used in different engineering disciplines [54–57].

MFO, proposed by Mirjalili [58], is an innovative MHA that draws inspiration from the intriguing behaviour of moths attracted to flames. MFO incorporates the unique phenomenon of moths spiralling around a flame into its search strategy. This behaviour, while seemingly irrational and perilous for the moths, serves as a metaphor for E&E in optimisation problems. MFO leverages a chaotic search mechanism that emulates the unpredictable flight patterns of moths around a flame. This mechanism enables the MFO to efficiently explore diverse solution spaces, avoiding stagnation in the local optima. By introducing chaos, the MFO promotes global exploration while maintaining its ability to exploit promising regions of the search space. The core idea behind MFO is to strike a balance between E&E, mimicking the trade-off faced by moths as they navigate the dangerous allure of flames. By dynamically adjusting the balance between E&E strategies, the MFO adaptively evolves its search behaviour, allowing it to effectively handle complex optimisation problems with varying landscapes. The effectiveness of MFO has been demonstrated across a wide range of applications, including engineering design, data mining, and image processing. Its ability to handle both continuous and discrete optimisation problems make it a versatile tool in the field of MHAs.

SMA [59] simulates the nutritive phase of a slime mould as a unique approach that is grounded in nature (a single-celled eukaryote). The foraging behaviour of slime moulds is simulated by this programme. By smelling potential food sources, slime moulds locate them, wrap them, and then digest them by secreting enzymes. In SMA, the phase of iterations to produce the highest smell concentration is the theoretical description of how

to approach the optimal solution. The slime mould's flexible weight ensures rapid convergence and prevents it from becoming stranded in regional extremes. This approach enables the slime mould to advance along any viable path in the direction of the ideal outcome, which mimics the slime mould's eating-related architecture. The next stage is wrapping the meal using contractions of the intravenous framework inside the upper and lower limitations. The vein with the maximum contraction of food generates more bio-oscillator waves, which cause the cytoplasm to flow more quickly through the vein, increasing its thickness. The search patterns in SMA are altered in response to the opposing signals from veins regarding the concentration of food.

MPA [60], a MHA inspired by the natural principles governing optimal foraging strategies and encounter rates between predator and prey in marine ecosystems. Marine predators adopt a Lévy strategy when navigating environments with scarce prey, while employing Brownian movement in areas abundant with prey. Throughout their lifetimes, these predators exhibit a consistent balance of Lévy and Brownian movement as they traverse diverse habitats. Environmental factors, such as eddy formation, influence their behaviour, prompting adaptive changes to explore regions with varying prey distributions. Leveraging their remarkable memory capabilities, they capitalise on the recollection of successful foraging locations and associations with other individuals. MPA harnesses these concepts to guide its search process, mimicking the adaptive foraging behaviour of marine predators. By integrating these nature-inspired mechanisms, MPA demonstrates a powerful optimisation approach capable of addressing complex problems in diverse domains.

Note that the detailed working principles of these OAs are not presented in this study because they are well established, and the original studies of MFO [58], SMA [59], and MPA [60] can be referred to for more details.

3.5. Hybrid Modelling of ANFIS and MHAs

In this work, the C&A parameters of ANFIS were optimised using MHAs. It is important to note that proper setting of the FIS and C&A parameters is necessary for creating an optimum ANFIS model because learning parameters have a significant impact on the model's performance. Notably, the selection of all of the ANFIS hyperparameters at once is a challenging operation because they must be searched in continuous domains, leading to an infinite number of parameters sets. As a result, it is possible to define the problem of ANFIS parameter tweaking as an optimisation problem. Thus, the values of the FIS and C&A parameters were optimised using IGWO, GWO, MFO, SMA, and MPA, and five hybrid ANFIS models, i.e., ANFIS-IGWO, ANFIS-GWO, ANFIS-MFO, ANFIS-SMA, and ANFIS-MPA, were created. A flow chart of the construction procedure of the hybrid ANFIS models is presented in Figure 2.

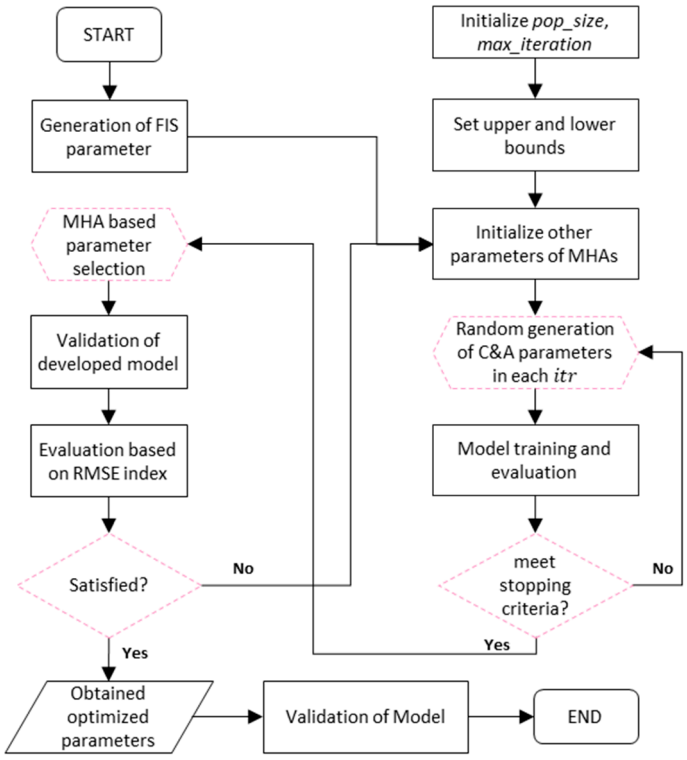

Figure 2. Flow chart of hybrid ANFIS model construction.

4. Data Description and Modelling

A broad variety of experimental results of soil compaction parameters were acquired from the studies of Günaydın [15], Wang and Yin [1], and Bardhan and Asteris [14]. Specifically, a total of 372 results were obtained, the details of which are presented in Table 1. The work of Günaydın [15] consists of 126 compaction results of nine distinct soil types (CH, CI, CL, GC, GM, MH, MI, ML, and SC) with six influencing parameters, viz., fines content (F), sand content (S), gravel content (G), specific gravity, liquid limit (LL), and plastic limit (PL). Wang and Yin [1] gathered a total of 226 records from the literature. The database includes G, S, F, LL, PL, and compaction energy of various soil types, such as CL, CL-ML, CH, MH, ML, SC, SP-SC, SW-SC, SM, GC, GP-GC, GW-GC, and GM. Bardhan and Asteris [14] presented 20 experimental records of soil compaction parameters, including four distinct soil types (CH, CI, CL, and SC) and six influencing parameters, identical to Günaydn [15]. According to the study of Wang and Yin [1], the majority of 226 soil compaction experiments were conducted using either the conventional Proctor or the reduced compaction energy. Additionally, thirty modified Proctor compaction tests were incorporated into the database.

Table 1. Details of data pre-processing for OMC and MDD estimation.

Particulars	No. of Actual Data	Actual Data Dimension	No. of Data Selected	Final Data Dimension
Günaydın [15]	126	126 × 8	126	126 × 7
Wang and Yin [1]	226	226 × 8	105	105 × 7
Bardhan and Asteris [14]	20	20 × 8	20	20 × 7
Final dataset (for this study)	-	-	251	251 × 7

Note: The data dimension also includes OMC and MDD parameters.

In this study, the database presented by Wang and Yin [1] has been revised, and a total of 105 records were chosen. Additionally, all datasets of Günaydın [15] and Bardhan and Asteris [14] were used. Therefore, 126, 105, and 20 experimental records were acquired from the studies of Günaydın [15], Wang and Yin [1], and Bardhan and Asteris [14], respectively.

The details of data dimension are also presented in Table 2. Therefore, the final database includes 251 records and five influential parameters viz., F in %, S in %, G in %, LL in %, and PL in %, of 15 different soil types. These five influential parameters were used to estimate the OMC and MDD of soils. Descriptive details of the final dataset are given in Table 2. In addition, the minimum and maximum values of influential (soil-type wise) and compaction parameters are presented in Table 3. Note that the abbreviations of soil types are presented as per the Indian Standard Soil Classification System (ISSCS) and ASTM [61].

Table 2. Descriptive statistics of the employed dataset.

Particulars	F (%)	S (%)	G (%)	LL (%)	PL (%)	OMC (%)	MDD (kN/m^3)
Min.	8.60	0.00	0.00	16.00	6.10	7.00	13.73
Avg.	63.76	27.95	8.29	40.14	20.63	17.16	17.25
Max.	100.00	83.60	67.10	70.00	32.50	31.00	21.48
Stnd. Error	1.49	1.09	0.74	0.63	0.28	0.24	0.08
Stnd. Dev.	23.62	17.19	11.78	9.93	4.50	3.87	1.29
Variance	557.68	295.50	138.65	98.62	20.21	15.00	1.67
Kurtosis	−0.90	−0.31	3.55	0.20	0.15	0.87	0.54
Skewness	−0.20	0.33	1.85	0.67	−0.06	0.38	0.02

Table 3. Soil type-wise details of the employed dataset.

Soil Types	F		S		G		LL		PL		OMC		MDD	
	Min.	Max.	Min.	Max.	Min.	Max.	Min.	Max.	Min.	Max.	Min.	Max.	Min.	Max.
CH	53.80	100.00	0.00	41.16	0.00	20.00	50.00	70.00	18.00	31.00	17.50	30.80	13.93	17.42
CI	49.00	75.00	21.00	44.95	0.05	23.07	35.15	49.40	14.40	26.72	13.95	23.75	15.19	19.41
CL	33.00	99.00	1.00	65.00	0.00	22.00	23.00	49.30	6.10	27.00	11.00	22.00	15.89	19.28
CL-ML	81.00	81.00	19.00	19.00	0.00	0.00	27.00	27.00	21.00	21.00	17.00	17.00	17.46	17.46
GC	13.00	41.50	19.90	45.61	30.39	67.10	27.60	63.20	13.40	26.11	7.60	18.80	16.43	20.51
GM	40.00	50.00	17.25	28.69	24.69	37.75	40.20	50.90	26.00	26.61	13.85	20.40	16.36	17.55
GP-GC	9.40	9.40	41.90	41.90	48.70	48.70	37.80	37.80	14.70	14.70	8.40	8.40	20.60	20.60
GW-GC	8.60	8.60	44.30	44.30	47.10	47.10	29.50	29.50	14.10	14.10	7.00	7.00	21.48	21.48
MH	60.00	100.00	0.00	36.48	0.00	3.52	50.40	64.00	26.00	32.50	19.40	31.00	13.73	16.09
MI	59.00	74.00	24.24	34.61	1.76	6.39	47.90	49.35	28.41	28.85	18.00	21.95	16.36	16.39
ML	53.00	90.00	10.00	37.00	0.00	10.00	25.00	47.00	14.55	28.00	10.40	22.00	15.89	19.24
SC	15.00	48.00	30.90	71.26	0.00	39.00	16.00	61.10	9.00	26.24	9.00	18.50	16.28	20.50
SM	44.00	44.00	56.00	56.00	0.00	0.00	16.00	16.00	9.00	9.00	9.00	9.00	20.01	20.01
SP-SC	8.80	8.80	83.60	83.60	7.60	7.60	31.20	31.20	19.30	19.30	10.80	10.80	19.13	19.13
SW-SC	9.60	9.60	77.30	77.30	13.10	13.10	30.40	30.40	18.80	18.80	9.80	9.80	19.72	19.72

Figure 3 shows the comparative histograms for each influential variable. To better illustrate, the correlation matrices between influential variables and compaction parameters are presented in Figure 4. From the information given in Table 2, Figures 3 and 4, it can be seen that the OMC has a negative correlation with the contents of S and G, whereas F, LL, and PL show a positive correlation. In contrast, F, LL, and PL exhibit negative correlations, while S and G contents have positive correlations with MDD. Notably, these figures are particularly useful, as they indicate the range of values of the parameters for which the reliability is limited, and further experimental investigation is required for values of the parameters included in these regions and not with the aim of updating the database in the future.

After finalising the database, it was divided into two subsets: a training (TR) subset that contained 80% of the overall dataset and a testing (TS) subset that contained the remaining 20% of the data. The following steps can be used to describe the computational modelling process for estimating soil compaction parameters: (a) choosing the main dataset; (b) data normalisation; (c) data partitioning and selection of TR and TS subsets; (d) model

construction using a training subset; (e) check model performance; (f) check terminating criteria; (g) model validation if terminating criteria are satisfied; and (h) performance assessment. The steps of computational modelling are illustrated in Figure 5.

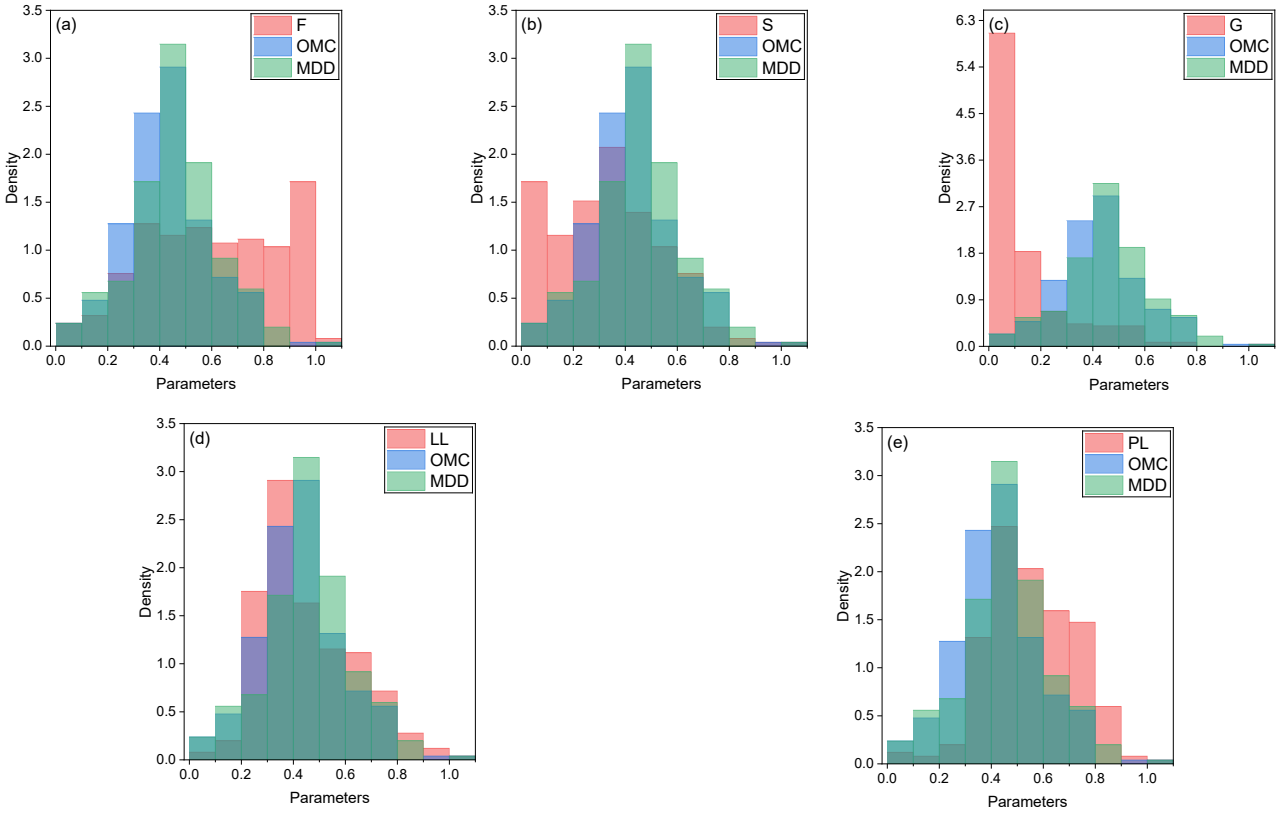

Figure 3. (**a**–**e**) Comparative histogram (values are in normalised form).

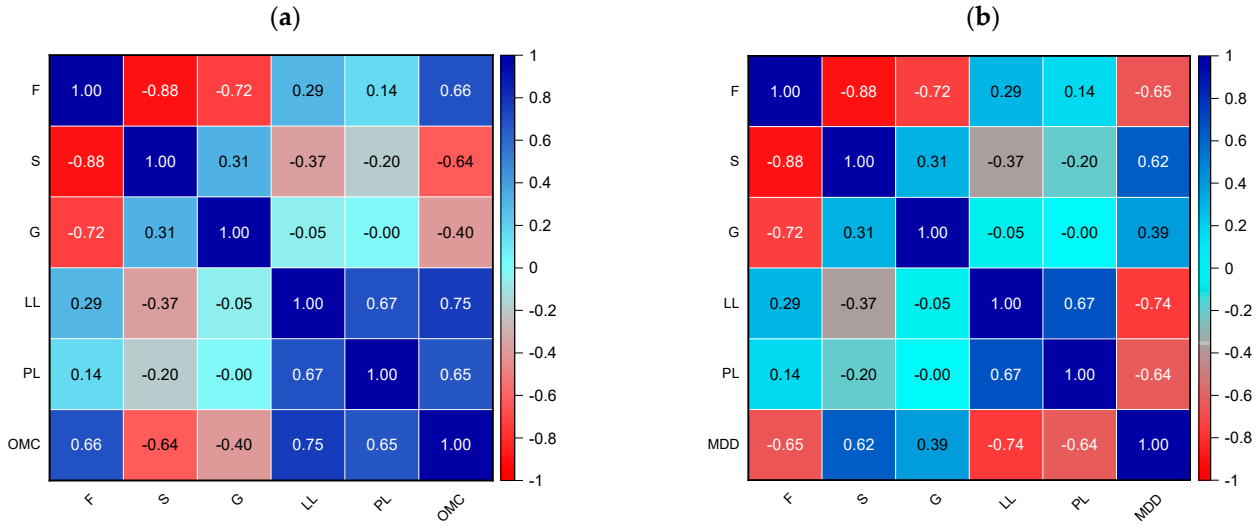

Figure 4. Correlation matrix between soil parameters and OMC (**a**) and MDD (**b**).

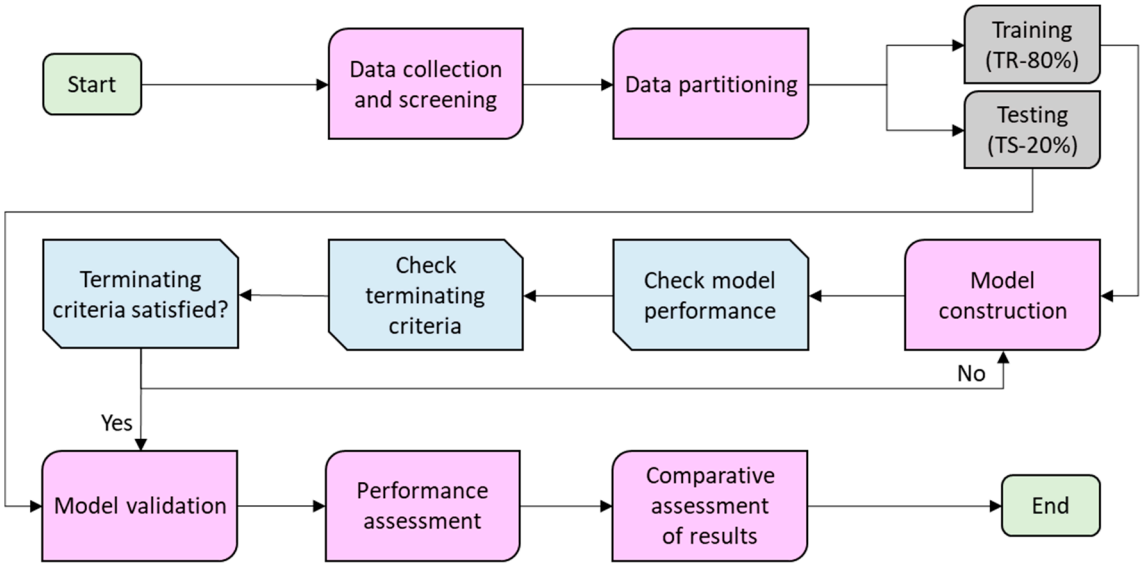

Figure 5. Steps of computational modelling.

5. Results and Discussion

The outcomes of the hybrid ANFIS models used to estimate soil compaction parameters are described in this section. As previously mentioned, the primary dataset was divided into training (201 samples) and testing (50 samples) subsets before the models were built. Note that all models were constructed and validated using identical training and testing subsets. The output of the developed models was then assessed using a number of indices, namely performance index (PFI), correlation coefficient (R), variance account factor (VAF), Willmott's Index of agreement (WI), mean absolute error (MAE), root mean square error (RMSE), RMSE to observation's standard deviation ratio (RSR), and weighted mean absolute percentage error (WMAPE). Notably, these indices are frequently used to evaluate the generalisability of any prediction model from a variety of perspectives, including correlation accuracy, related error, amount of variation, and so on.

In contrast, the deterministic parameters of MHAs, such as swarm size, maximum iteration number, and upper and lower bounds, play a vital part in hybrid modelling; thus, they were calibrated throughout the optimisation process. The details of the deterministic and hyper-parameters of hybrid ANFIS models in estimating soil compaction parameters are described in the following sub-section, followed by a comparative assessment of the results.

$$PFI = adj.R^2 + 0.01VAF - RMSE \tag{10}$$

$$R = \sqrt{\frac{\sum_{i=1}^{n}(y_i - y_{mean})^2 - \sum_{i=1}^{n}(y_i - \hat{y}_i)^2}{\sum_{i=1}^{n}(y_i - y_{mean})^2}} \tag{11}$$

$$VAF\ (\%) = \left(1 - \frac{var(y_i - \hat{y}_i)}{var(y_i)}\right) \times 100 \tag{12}$$

$$WI = 1 - \left[\frac{\sum_{i=1}^{n}(y_i - \hat{y}_i)^2}{\sum_{i=1}^{n}\{|\hat{y}_i - y_{mean}| + |y_i - y_{mean}|\}^2}\right] \tag{13}$$

$$MAE = \frac{1}{n}\sum_{i=1}^{n}|(\hat{y}_i - y_i)| \tag{14}$$

$$RMSE = \sqrt{\frac{1}{n}\sum_{i=1}^{n}(y_i - \hat{y}_i)^2} \tag{15}$$

$$RSR = \frac{RMSE}{\sqrt{\frac{1}{n}\sum_{i=1}^{n}(y_i - y_{mean})^2}} \quad (16)$$

$$WMAPE = \frac{\sum_{i=1}^{n}\left|\frac{y_i - \hat{y}_i}{y_i}\right| \times y_i}{\sum_{i=1}^{n} y_i} \quad (17)$$

where y_i = actual ith value; $\hat{y}_i$ = estimated ith value; n = is the number of samples; and y_{mean} = mean of the actual value. Note that for a perfect predictive model, the values of the aforementioned indices should be identical to their identical values, the details of which can be obtained from the literature [14,17].

5.1. Model Performance

The results of the hybrid ANFIS models that were built to estimate soil OMC and MDD are presented in this sub-section. As stated above, the optimum selection of hyper-parameters is a challenging operation, and hence, proper tuning of FIS and C&A parameters was performed during the course of hybrid modelling. The number of FIS parameters (N_{FIS}) were investigated between 2 and 15. Using Gaussian MF and RMSE as fitness functions, the most appropriate value of N_{FIS} was determined to be 5. Notably, Gaussian and linear MFs were used in the input and output layers, respectively. A total of 60 C&A membership functions of ANFIS were optimised for the nine-dimensional input space. Note that the optimised values of N_{FIS} and C&A were chosen following a trial-and-error approach and according to the performance during the testing phase. The convergence behaviour and computational time of the developed hybrid ANFIS models are presented in Figures 6 and 7, respectively. It should be noted that the computational time of the developed ANFIS-IGWO model was found to be longer due to the use of an upgraded version of GWO that required changed mathematical calculations to handle E&E operations. Moreover, it is seen that all the developed hybrid models converge within 500 epochs; hence, they are considered to be sufficient as the maximum iteration count.

The performance of the developed ANFIS models is presented in Tables 4 and 5, respectively, for the OMC and MDD estimations. The abilities of the constructed models for training, testing, and total outputs are shown here. It should be underlined that the training subset performance was used to define the goodness of fit of the developed models, while the testing dataset was used to evaluate their generalisation potential. According to Table 4, it is seen that the developed ANFIS-MPA achieved the highest R and lowest RMSE values of 0.9335 and 0.0590, respectively, during the training phase of OMC prediction. However, during the testing phase, the constructed ANFIS-IGWO achieved the most precise precision, with R = 0.8645 and RMSE = 0.0754. According to the overall results of the OMC estimation, the ANFIS-IGWO was determined to be the best-fitted model with R = 0.9203 and RMSE = 0.0635, followed by ANFIS-MFO (R = 0.9191 and RMSE = 0.0636), ANFIS-GWO (R = 0.9167 and RMSE = 0.0647), and ANFIS-MPA (R = 0.9153 and RMSE = 0.0652). The developed ANFIS-SMA model was the least performing model, with R = 0.9139 (lowest among other developed models) and RMSE = 0.0658 (highest among other developed models).

On the contrary, the results of Table 5 exhibit that the developed ANFIS-MPA (R = 0.9142 and RMSE = 0.0692) and ANFIS-MFO (R = 0.9131 and RMSE = 0.0697) models were found to be the top-two models during the training phase of MDD estimation, while the constructed ANFIS-IGWO (R = 0.8619 and RMSE = 0.0738) and ANFIS-GWO (R = 0.8562 and RMSE = 0.0749) models were found to be the best-two models in the testing phase. According to the overall results of the MDD estimation, the ANFIS-IGWO was determined to be the best-fitted model with R = 0.9050 and RMSE = 0.0709, followed by ANFIS-GWO (R = 0.8973 and RMSE = 0.0735), ANFIS-SMA (R = 0.8964 and RMSE = 0.0739), and ANFIS-MFO (R = 0.8935 and RMSE = 0.0752). The developed ANFIS-MPA model was the least performing model, with R = 0.8866 (lowest among other developed models) and

RMSE = 0.0774 (highest among other developed models). These findings demonstrate the good predictive performance of the suggested ANFIS-IGWO model during both the OMC and MDD predictions.

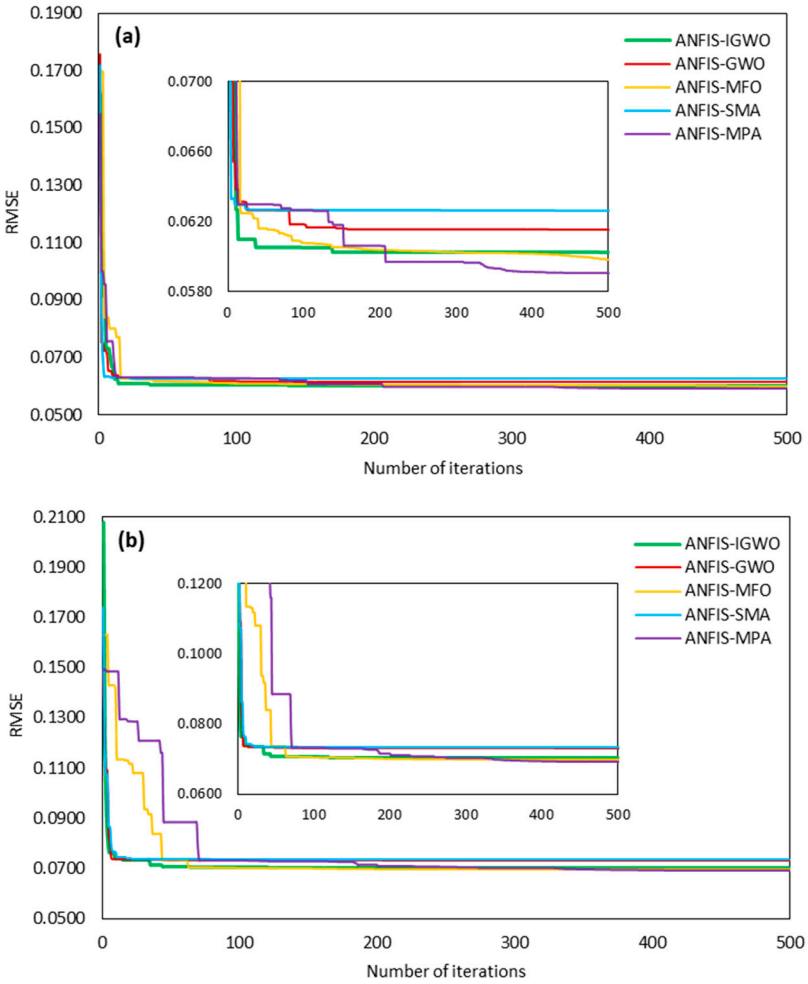

Figure 6. Convergence curve of the developed hybrid ANFIS models for (**a**) OMC and (**b**) MDD estimations.

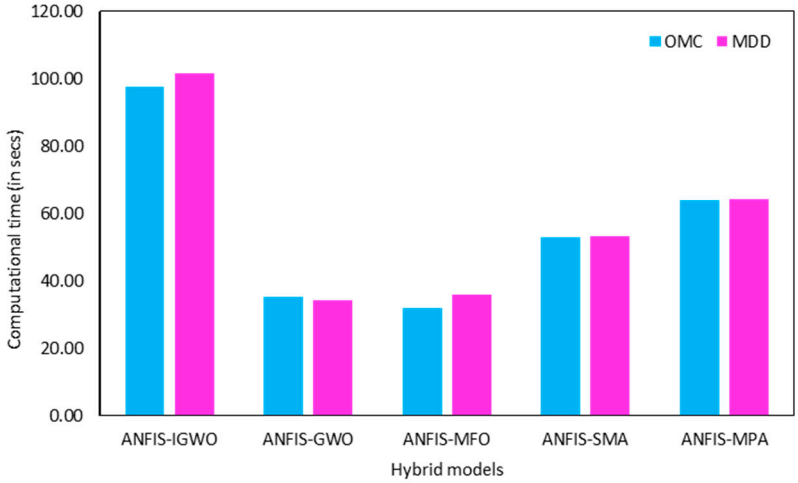

Figure 7. Illustration of the computational time of the developed hybrid ANFIS models.

Table 4. Performance indices for OMC prediction.

Phases	Models	PFI	R	VAF	WI	MAE	RMSE	RSR	WMAPE
Training	ANFIS-IGWO	1.6686	0.9307	86.5973	0.9636	0.0479	0.0602	0.3662	0.1088
	ANFIS-GWO	1.6550	0.9274	86.0065	0.9610	0.0473	0.0615	0.3741	0.1081
	ANFIS-MFO	1.6757	0.9328	86.8809	0.9622	0.0453	0.0598	0.3636	0.1036
	ANFIS-SMA	1.6439	0.9247	85.5093	0.9594	0.0487	0.0626	0.3808	0.1106
	ANFIS-MPA	**1.6801**	**0.9335**	**87.1078**	**0.9638**	**0.0449**	**0.0590**	**0.3591**	**0.1025**
Testing	ANFIS-IGWO	**1.3766**	**0.8645**	73.3267	**0.9167**	0.0604	**0.0754**	**0.5607**	0.1627
	ANFIS-GWO	1.3726	0.8625	**73.3937**	0.9132	0.0602	0.0762	0.5666	0.1623
	ANFIS-MFO	1.3494	0.8560	72.4010	0.9107	**0.0584**	0.0770	0.5729	**0.1573**
	ANFIS-SMA	1.3526	0.8604	71.9109	0.9143	0.0625	0.0772	0.5742	0.1683
	ANFIS-MPA	1.2137	0.8395	62.7992	0.9041	0.0641	0.0854	0.6353	0.1726
Total	ANFIS-IGWO	**1.6265**	**0.9203**	**84.6266**	**0.9577**	0.0504	**0.0635**	**0.3932**	0.1182
	ANFIS-GWO	1.6125	0.9167	84.0233	0.9549	0.0499	0.0647	0.4004	0.1176
	ANFIS-MFO	1.6222	0.9191	84.4224	0.9555	**0.0479**	0.0636	0.3936	**0.1130**
	ANFIS-SMA	1.6012	0.9139	83.5102	0.9536	0.0515	0.0658	0.4071	0.1207
	ANFIS-MPA	1.6066	0.9153	83.7206	0.9551	0.0488	0.0652	0.4032	0.1147

Note: Bold values indicate best-obtained performance.

Table 5. Performance indices for MDD prediction.

Phases	Models	PFI	R	VAF	WI	MAE	RMSE	RSR	WMAPE
Training	ANFIS-IGWO	1.5872	0.9116	83.0798	0.9526	0.0540	0.0702	0.4114	0.1202
	ANFIS-GWO	1.5551	0.9036	81.6465	0.9471	0.0559	0.0731	0.4284	0.1243
	ANFIS-MFO	1.5933	0.9131	83.3592	0.9532	0.0529	0.0697	0.4085	0.1178
	ANFIS-SMA	1.5528	0.9030	81.5383	0.9464	0.0564	0.0734	0.4300	0.1256
	ANFIS-MPA	**1.5981**	**0.9142**	**83.5737**	**0.9535**	**0.0522**	**0.0692**	**0.4053**	**0.1160**
Testing	ANFIS-IGWO	**1.3740**	**0.8619**	**73.4131**	**0.9244**	**0.0620**	**0.0738**	**0.5229**	**0.1257**
	ANFIS-GWO	1.3524	0.8562	72.4607	0.9213	0.0636	0.0749	0.5308	0.1291
	ANFIS-MFO	1.0522	0.7831	57.7198	0.8794	0.0709	0.0943	0.6679	0.1438
	ANFIS-SMA	1.3428	0.8538	72.0656	0.9189	0.0646	0.0759	0.5381	0.1311
	ANFIS-MPA	0.8772	0.7560	45.8550	0.8642	0.0771	0.1042	0.7382	0.1564
Total	ANFIS-IGWO	**1.5630**	**0.9050**	**81.8582**	**0.9493**	**0.0556**	**0.0709**	**0.4256**	**0.1214**
	ANFIS-GWO	1.5328	0.8973	80.5090	0.9442	0.0574	0.0735	0.4407	0.1254
	ANFIS-MFO	1.5161	0.8935	79.7219	0.9429	0.0565	0.0752	0.4514	0.1234
	ANFIS-SMA	1.5292	0.8964	80.3568	0.9431	0.0580	0.0739	0.4433	0.1268
	ANFIS-MPA	1.4878	0.8866	78.3472	0.9401	0.0571	0.0774	0.4644	0.1247

Note: Bold values indicate best-obtained performance.

To better demonstrate the performance of the developed ANFIS models, scatterplots are presented in Figures 8 and 9 for the OMC and MDD estimations, respectively. Herein, the illustrations of actual and estimated values for the best three models (based on RMSE value) are shown. The amount of variance in these diagrams can be visualised by viewing red-coloured dotted lines put at 10% levels. The performance of the generated hybrid models is compared in the following sub-section, and a comparative assessment is presented using a variety of graphical illustrations.

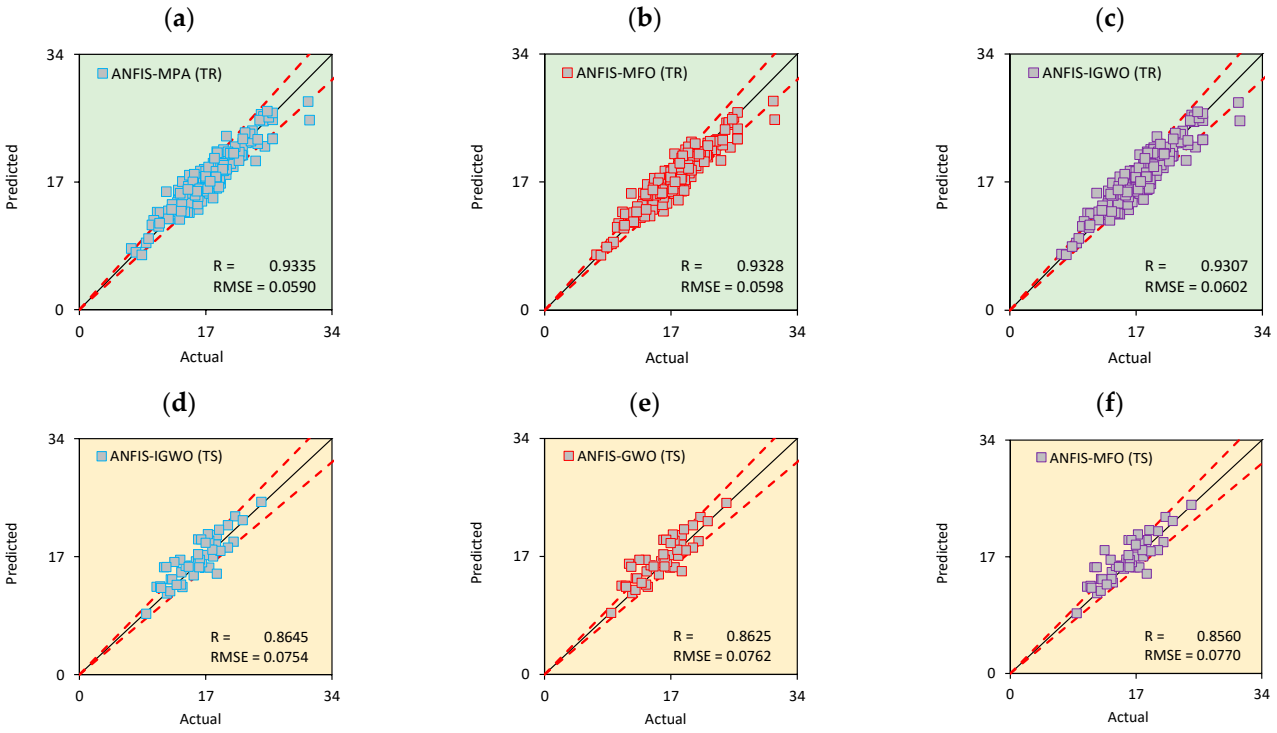

Figure 8. Scatter plot of OMC prediction for the best three models (based on RMSE index) in (**a**–**c**) training and (**d**–**f**) testing phases.

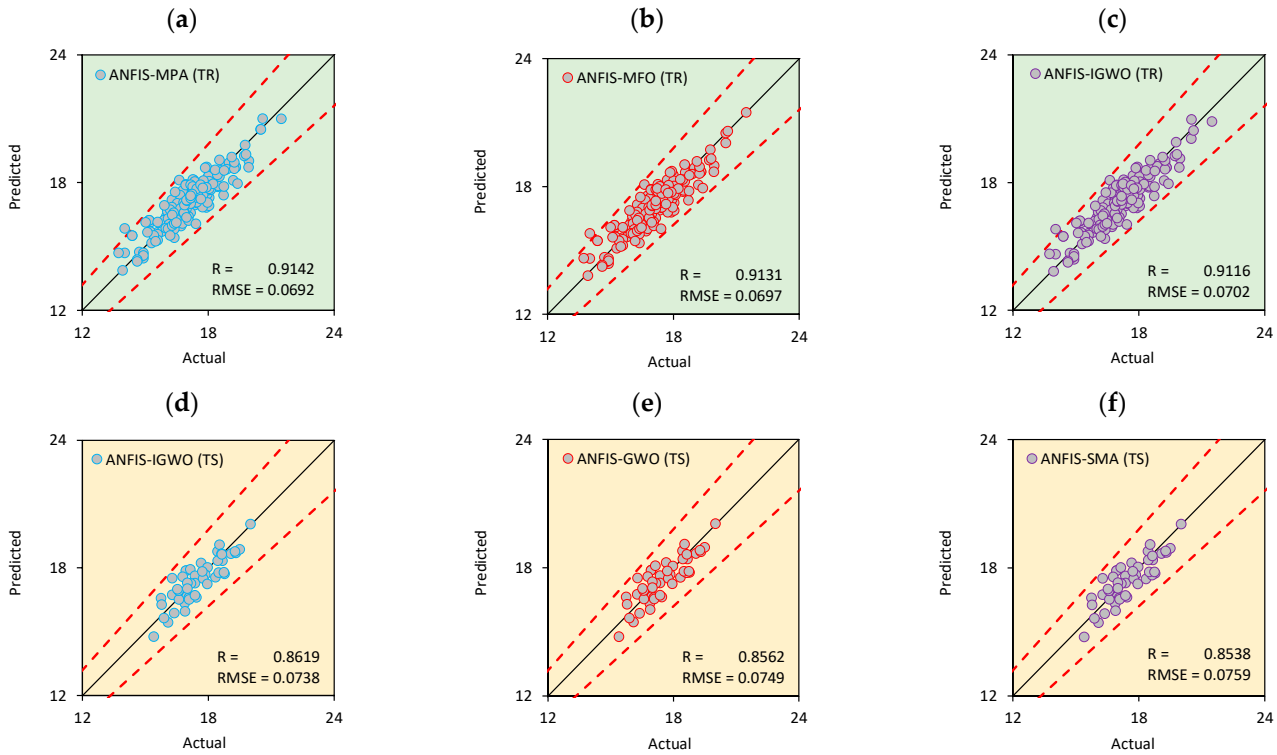

Figure 9. Scatter plot of MDD prediction for the best three models (based on RMSE index) in (**a**–**c**) training and (**d**–**f**) testing phases.

5.2. Discussion of Results

It is critical to highlight that a data-driven model is incomplete without a visual representation of the results. Visualisations enable the identification of the degree of accuracy and associated errors in a model that is easier to comprehend. Therefore, the results are displayed in the form of an accuracy matrix, Taylor diagrams, and radar plots. Notably, the Taylor diagrams are shown for the testing dataset only, since the performance of a data-driven model during the testing dataset should be accepted with more certainty. For thoroughly assessing a model's overall correctness, these diagrams are quite beneficial. An accuracy matrix is a heat map matrix that is used to measure the level of accuracy that a model achieves in terms of certain performance criteria. This matrix makes it simple to evaluate a model's correctness without having to look up each index's value. As previously stated, a number of indices must be created to assess a model's accuracy from multiple angles; however, interpreting results by looking at each index's values takes time and necessitates in-depth observation. Figure 10 shows the accuracy matrix for the models created for the OMC and MDD predictions. The accuracy matrix demonstrates that the constructed ANFIS-IGWO attained higher predictive precision against each index during the testing phase.

On the other hand, the Taylor diagram [62] is used to provide a quick assessment of a model's accuracy in terms of the coefficient of correlation, ratio of standard deviations, and RMSE index. Generally, a point inside a Taylor diagram indicates a model. The position of the point should line up with the reference point for an ideal model. The Taylor diagrams for the hybrid ANFIS models developed for OMC and MDD predictions are shown in Figure 11. In addition to the accuracy matrix and Taylor diagrams, radar plots representing the R value are also presented in Figure 12 for the training, testing, and total cases of OMC and MDD estimations. A ridgeline chart and distribution with Kernel smooth of error between actual and estimated values are presented in Figure 13. From these diagrams, the predictive capability of hybrid ANFIS models can be assessed from different perspectives.

However, according to the aforementioned results, the ANFIS-IGWO model was found to be the best-obtained model in both instances of prediction. As indicated previously, eight indices were used to evaluate the performance of the developed ANFIS models. Based on the overall results against OMC prediction, the developed ANFIS-IGWO achieved the highest level of accuracy, with R = 0.9203 and RMSE = 0.0635, whereas against MDD prediction, R = 0.9050 and RMSE = 0.0709 achieved the highest level of accuracy. Therefore, the suggested ANFIS-IGWO model can be used to approximate the OMC and MDD ranges for various soil types. This will aid engineers and practitioners in reducing the operational time required for laboratory compaction experiments. The developed MATLAB models, as well as the employed dataset, are included as Supplementary Materials for future use. The details of MATLAB implementations of the developed models are also presented in Appendix A. For better demonstration, the steps of OMC and MDD estimations using basic soil parameters and the developed MATLAB models are illustrated in Figure 14.

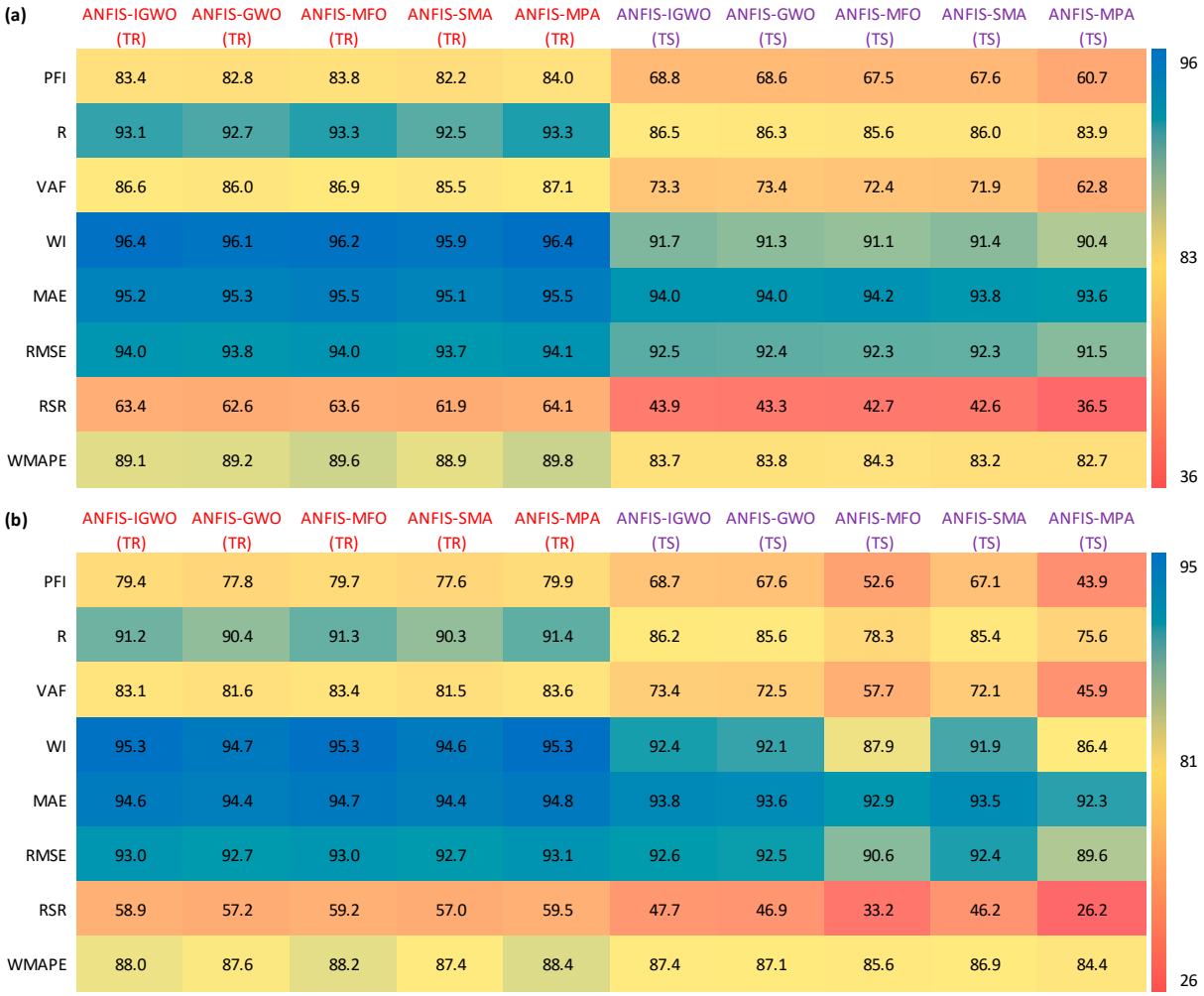

Figure 10. Accuracy matrix (testing phase) for (**a**) OMC and (**b**) MDD predictions.

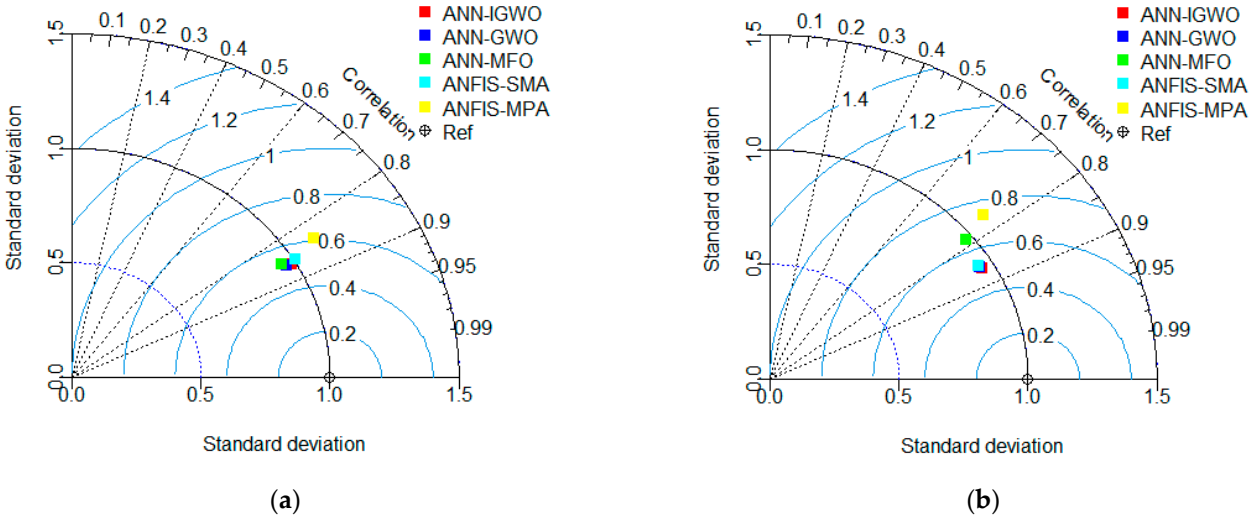

Figure 11. Taylor diagram (testing phase) for (**a**) OMC and (**b**) MDD predictions.

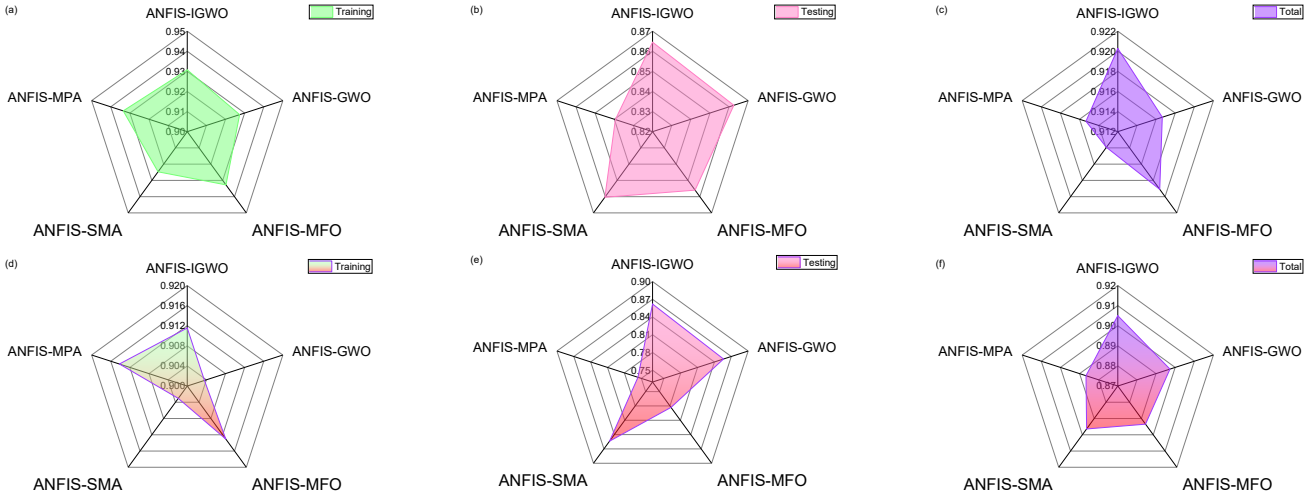

Figure 12. Radar plot representing the R value for (**a**–**c**) OMC and (**d**–**f**) MDD predictions.

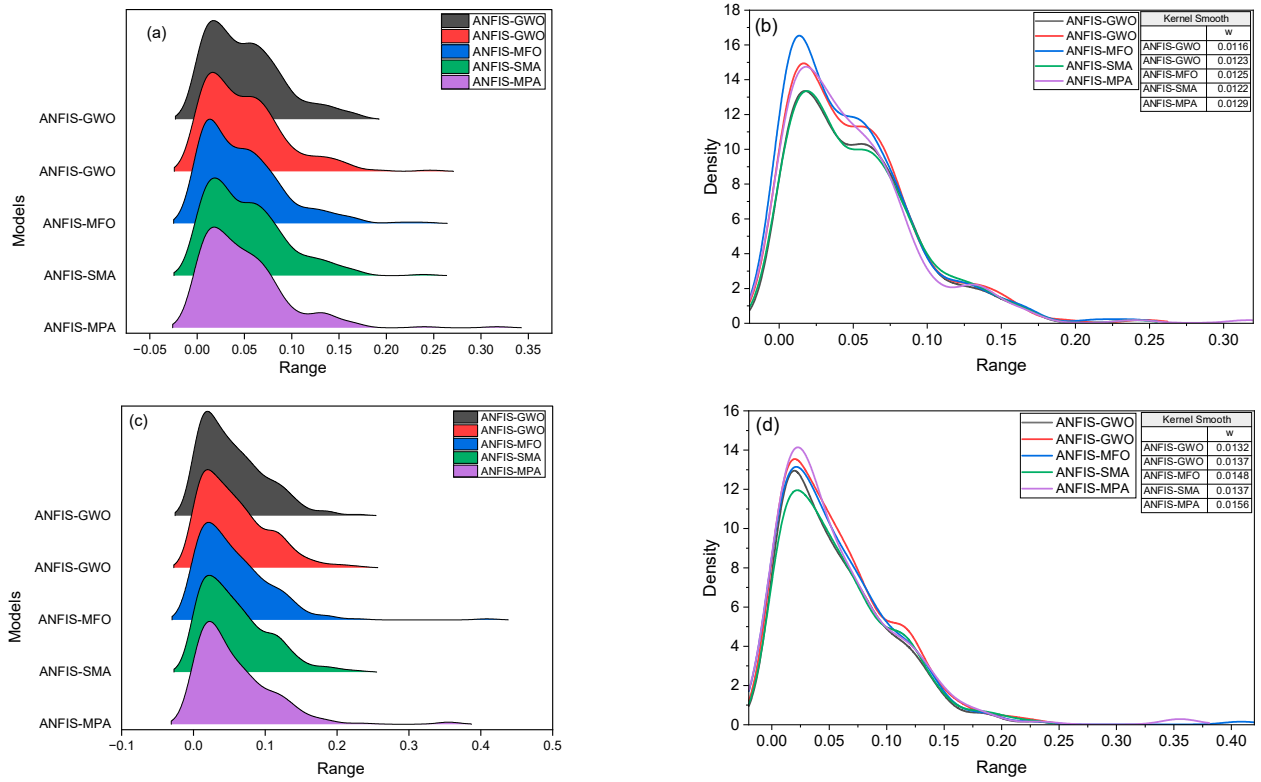

Figure 13. Ridgeline chart (left) and distribution with Kernel smooth (right) plots for (**a**,**b**) OMC and (**c**,**d**) MDD predictions.

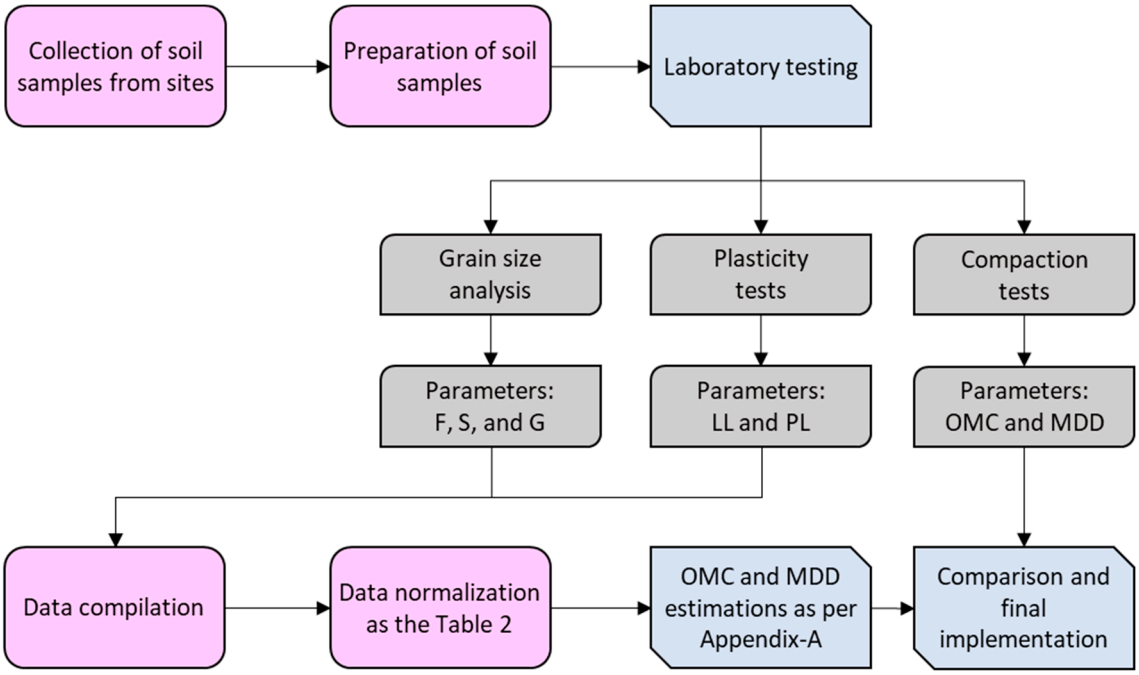

Figure 14. Illustration of the steps of OMC and MDD estimations using basic soil parameters and the developed MATLAB models.

6. Limitations and Future Research

In this section, the limitations of the proposed ANFIS-IGWO model are presented, as well as the main points that need to be further investigated. Regarding the estimation of the OMC and MDD of soils, it is worth noting that despite the excellent prediction it achieves, and which are presented in the previous section, it only applies to values of the input parameters between the minimum and the maximum values (refer to Table 2) that have the corresponding parameters of the database used to train and develop the model. Additionally, the reliability of the proposed model is limited for parameter value ranges, where the number of experimental data and soil types are not sufficient. That is, in cases in which the number of data is very small, and thus unable to satisfactorily describe the soil compaction. For example, based on the histograms of Figure 3, it was found that there is not enough data in some regions. Such value ranges, where there is a shortage of each of the input parameters, should be studied experimentally in the near future and updated the database with the aim of future development of more efficient forecasting soft computing models.

7. Summary and Conclusions

Soil compaction parameters play a vital role in construction projects. They are crucial for comparing the level of compaction achieved in the field. However, the traditional laboratory method for determining OMC and MDD is time consuming. Therefore, the main objective of this study is to sidestep the need for multiple laboratory tests by leveraging the predictive capabilities of high-performance hybrid intelligence paradigms. Taking these points into consideration, the current study proposes a high-performance hybrid model to sidestep the operation of typical laboratory testing of soil compaction parameters. To achieve this goal, an ANFIS-IGWO model was constructed, and the performance of this model was compared with four hybrid ANFIS models, namely ANFIS-GWO, ANFIS-MFO, ANFIS-SMA, and ANFIS-MPA. The experimental results clearly demonstrate that the proposed ANFIS-IGWO model effectively predicts soil compaction parameters. With an accuracy range of 92.5% to 94%, according to the RMSE index, the developed ANFIS-IGWO model exhibits superior generalisation abilities for estimating soil compaction parameters.

According to the overall outcomes, the proposed ANFIS-IGWO model offers a significant advantage by transforming the C&A parameters of the model into the coordinates of individual wolves within the community. Each wolf's position represents a result of the ANFIS-IGWO model, with N_{FIS} = 5 and 500 epochs utilised. However, a drawback of the ANFIS-IGWO model is its high computational cost due to the implementation of a modified approach. Multiple runs were performed to identify the most suitable search space for accurate output estimation, further increasing the time required. Other limitations encompass no external validation performed and the exclusion of factors such as compaction energy and the parental significance of soils during modelling. Therefore, additional research is needed to expand the application of the suggested ANFIS-IGWO model in estimating soil compaction parameters. Future directions should involve (a) a comprehensive assessment of the model's superiority using real-life data from diverse construction sites; (b) external validation using a real-life database of different soil types; (c) consideration of compaction energy as an influencing variable; (d) the implementation of newly introduced MHAs and their improved/enhanced, and (e) a comprehensive analysis of hybrid and traditional ANFIS paradigms in estimating soil compaction parameters. Nevertheless, the employed dataset and the MATLAB models developed in this study are provided as Supplementary Materials to encourage further research.

Supplementary Materials: The following supporting information can be downloaded at: https://www.mdpi.com/article/10.3390/math11143064/s1.

Author Contributions: Conceptualisation, A.B.; methodology, A.B.; software, A.B. and P.G.A.; formal analysis, A.B.; validation, G.K.; writing—original draft preparation, A.B., R.K.S., S.G. and G.K.; writing—review and editing, A.B. and P.G.A. All authors have read and agreed to the published version of the manuscript.

Funding: This research received no external funding.

Data Availability Statement: Attached as a Supplementary Materials.

Conflicts of Interest: The authors declare no conflict of interest.

Nomenclature

ANFIS	Adaptive neuro-fuzzy inference system	MF	Membership function
ANFIS-GWO	Hybrid model of ANFIS and GWO	MFO	Moth-flame optimisation
ANFIS-IGWO	Hybrid model of ANFIS and IGWO	MHA	Meta-heuristic algorithm
ANFIS-MFO	Hybrid model of ANFIS and MFO	MLT	Machine learning technique
ANFIS-MPA	Hybrid model of ANFIS and MPA	MPA	Marine predators algorithm
ANFIS-SMA	Hybrid model of ANFIS and SMA	N_{FIS}	Number of FIS parameters
ANN	Artificial neural network	OMC	Optimum moisture content
C&A	Consequent and antecedent	PFI	Performance index
E&E	Exploration and exploitation	PL	Plastic limit
ELM	Extreme learning machine	R	Correlation coefficient
EPR	Evolutionary polynomial regression	R^2	Determination coefficient
F	Fines content	RMSE	Root mean square error
FIS	Fuzzy inference system	RSR	RMSE to observation's standard deviation ratio
G	Gravel content	S	Sand content
GMDH	Group method of data handling	SMA	Slime mould algorithm
GWO	Grey wolf optimiser	SVM	Support vector machine
IGWO	Improved grey wolf optimiser	TR	Training subset
LL	Liquid limit	TS	Testing subset

LSSVM	Least square support vector machine	VAF	Variance account factor
MAE	Mean absolute error	WI	Willmott's Index of agreement
MDD	Maximum dry density	WMAPE	Weighted mean absolute percentage error

Appendix A

- MATLAB implementation for the developed ANFIS-IGWO model.

%% Dataset uploading: For dataset uploading via an Excel sheet named 'PROJECT.' The training dataset should be kept in the TR sheet, and the testing dataset should be kept in the TS sheet. The output value should be placed in the right-most column. All the values are given in normalised form.

```
train=xlsread('PROJECT', 'TR');
test=xlsread('PROJECT', 'TS');
xtrain = train(:,1:end-1); ytrain = train(:,end);
xtest = test(:,1:end-1); ytest = test(:,end);

%% Loading of the ANFIS-IGWO model for OMC estimation
%% Loading of anfis_igwo_mdd is necessary for MDD estimation

load anfis_igwo_omc
load anfis_igwo_mdd

%% Prediction of training and testing outputs (normalised values)

Pr_train_norm=evalfis(xtrain,fis);
Pr_test_norm=evalfis(xtest,fis);

%% Generation of de-normalisation values of OMC

Pr_train_act=(Pr_train_norm*24) + 7;
Pr_test_act=(Pr_test_norm*24) + 7;

%% Generation of de-normalisation values of MDD

Pr_train_act=(Pr_train_norm*7.7499) + 13.7340;
Pr_test_act=(Pr_test_norm*7.7499) + 13.7340;
```

References

1. Wang, H.-L.; Yin, Z.-Y. High performance prediction of soil compaction parameters using multi expression programming. *Eng. Geol.* **2020**, *276*, 105758. [CrossRef]
2. Tatsuoka, F.; Correia, A.G. Importance of controlling the degree of saturation in soil compaction linked to soil structure design. *Transp. Geotech.* **2018**, *17*, 3–23. [CrossRef]
3. Proctor, R. Fundamental principles of soil compaction. *Eng. News Record.* **1933**, *111*.
4. Xu, C.; Chen, Z.; Li, J.; Xiao, Y. Compaction of subgrade by high-energy impact rollers on an airport runway. *J. Perform. Constr. Facil.* **2014**, *28*, 4014021. [CrossRef]
5. Chen, R.-P.; Qi, S.; Wang, H.-L.; Cui, Y.-J. Microstructure and hydraulic properties of coarse-grained subgrade soil used in high-speed railway at various compaction degrees. *J. Mater. Civ. Eng.* **2019**, *31*, 4019301. [CrossRef]
6. Xu, Z.; Li, X.; Li, J.; Xue, Y.; Jiang, S.; Liu, L.; Luo, Q.; Wu, K.; Zhang, N.; Feng, Y. Characteristics of source rocks and genetic origins of natural gas in deep formations, Gudian Depression, Songliao Basin, NE China. *ACS Earth Space Chem.* **2022**, *6*, 1750–1771. [CrossRef]
7. Wu, Z.; Xu, J.; Li, Y.; Wang, S. Disturbed state concept–based model for the uniaxial strain-softening behavior of fiber-reinforced soil. *Int. J. Geomech.* **2022**, *22*, 4022092. [CrossRef]

8. Ren, C.; Yu, J.; Liu, S.; Yao, W.; Zhu, Y.; Liu, X. A plastic strain-induced damage model of porous rock suitable for different stress paths. *Rock Mech. Rock Eng.* **2022**, *55*, 1887–1906. [CrossRef]
9. Najjar, Y.M.; Basheer, I.A.; Naouss, W.A. On the identification of compaction characteristics by neuronets. *Comput. Geotech.* **1996**, *18*, 167–187. [CrossRef]
10. Nagaraj, H.B.; Reesha, B.; Sravan, M.V.; Suresh, M.R. Correlation of compaction characteristics of natural soils with modified plastic limit. *Transp. Geotech.* **2015**, *2*, 65–77. [CrossRef]
11. Peng, J.; Xu, C.; Dai, B.; Sun, L.; Feng, J.; Huang, Q. Numerical investigation of brittleness effect on strength and microcracking behavior of crystalline rock. *Int. J. Geomech.* **2022**, *22*, 4022178. [CrossRef]
12. Fu, Q.; Gu, M.; Yuan, J.; Lin, Y. Experimental study on vibration velocity of piled raft supported embankment and foundation for ballastless high speed railway. *Buildings* **2022**, *12*, 1982. [CrossRef]
13. Cheng, F.; Li, J.; Zhou, L.; Lin, G. Fragility analysis of nuclear power plant structure under real and spectrum-compatible seismic waves considering soil-structure interaction effect. *Eng. Struct.* **2023**, *280*, 115684. [CrossRef]
14. Bardhan, A.; Asteris, P.G. Application of hybrid ANN paradigms built with nature inspired meta-heuristics for modelling soil compaction parameters. *Transp. Geotech.* **2023**, *41*, 100995. [CrossRef]
15. Günaydın, O. Estimation of soil compaction parameters by using statistical analyses and artificial neural networks. *Environ. Geol.* **2009**, *57*, 203–215. [CrossRef]
16. Kurnaz, T.F.; Kaya, Y. The performance comparison of the soft computing methods on the prediction of soil compaction parameters. *Arab. J. Geosci.* **2020**, *13*, 159. [CrossRef]
17. Tiwari, L.B.; Burman, A.; Samui, P. Modelling soil compaction parameters using a hybrid soft computing technique of LSSVM and symbiotic organisms search. *Innov. Infrastruct. Solut.* **2023**, *8*, 2. [CrossRef]
18. Sinha, S.K.; Wang, M.C. Artificial neural network prediction models for soil compaction and permeability. *Geotech. Geol. Eng.* **2008**, *26*, 47–64. [CrossRef]
19. Ardakani, A.; Kordnaeij, A. Soil compaction parameters prediction using GMDH-type neural network and genetic algorithm. *Eur. J. Environ. Civ. Eng.* **2019**, *23*, 449–462. [CrossRef]
20. Yu, J.; Zhu, Y.; Yao, W.; Liu, X.; Ren, C.; Cai, Y.; Tang, X. Stress relaxation behaviour of marble under cyclic weak disturbance and confining pressures. *Measurement* **2021**, *182*, 109777. [CrossRef]
21. Wang, W.; Li, D.-Q.; Tang, X.-S.; Du, W. Seismic fragility and demand hazard analyses for earth slopes incorporating soil property variability. *Soil Dyn. Earthq. Eng.* **2023**, *173*, 108088. [CrossRef]
22. Ran, C.; Bai, X.; Tan, Q.; Luo, G.; Cao, Y.; Wu, L.; Chen, F.; Li, C.; Luo, X.; Liu, M. Threat of soil formation rate to health of karst ecosystem. *Sci. Total Environ.* **2023**, *887*, 163911. [CrossRef] [PubMed]
23. Liu, Y.; Li, J.; Lin, G. Seismic performance of advanced three-dimensional base-isolated nuclear structures in complex-layered sites. *Eng. Struct.* **2023**, *289*, 116247. [CrossRef]
24. Bui, D.T.; Nhu, V.-H.; Hoang, N.-D. Prediction of soil compression coefficient for urban housing project using novel integration machine learning approach of swarm intelligence and multi-layer perceptron neural network. *Adv. Eng. Inform.* **2018**, *38*, 593–604.
25. Truong, V.-H.; Pham, H.-A.; Van, T.H.; Tangaramvong, S. Evaluation of machine learning models for load-carrying capacity assessment of semi-rigid steel structures. *Eng. Struct.* **2022**, *273*, 115001. [CrossRef]
26. Truong, V.-H.; Papazafeiropoulos, G.; Vu, Q.-V.; Pham, V.-T.; Kong, Z. Predicting the patch load resistance of stiffened plate girders using machine learning algorithms. *Ocean Eng.* **2021**, *240*, 109886. [CrossRef]
27. Benbouras, M.A.; Lefilef, L. Progressive machine learning approaches for predicting the soil compaction parameters. *Transp. Infrastruct. Geotechnol.* **2023**, *10*, 211–238. [CrossRef]
28. Golafshani, E.M.; Behnood, A.; Arashpour, M. Predicting the compressive strength of normal and High-Performance Concretes using ANN and ANFIS hybridized with Grey Wolf Optimizer. *Constr. Build. Mater.* **2020**, *232*, 117266. [CrossRef]
29. Le, L.T.; Nguyen, H.; Dou, J.; Zhou, J. A comparative study of PSO-ANN, GA-ANN, ICA-ANN, and ABC-ANN in estimating the heating load of buildings' energy efficiency for smart city planning. *Appl. Sci.* **2019**, *9*, 2630. [CrossRef]
30. Piro, N.S.; Mohammed, A.; Hamad, S.M.; Kurda, R. Artificial neural networks (ANN), MARS, and adaptive network-based fuzzy inference system (ANFIS) to predict the stress at the failure of concrete with waste steel slag coarse aggregate replacement. *Neural Comput. Appl.* **2023**, *35*, 13293–13319. [CrossRef]
31. Ojha, V.K.; Abraham, A.; Snášel, V. Metaheuristic design of feedforward neural networks: A review of two decades of research. *Eng. Appl. Artif. Intell.* **2017**, *60*, 97–116. [CrossRef]
32. Behnood, A.; Golafshani, E.M. Predicting the compressive strength of silica fume concrete using hybrid artificial neural network with multi-objective grey wolves. *J. Clean. Prod.* **2018**, *202*, 54–64. [CrossRef]
33. Ly, H.-B.; Pham, B.T.; Le, L.M.; Le, T.-T.; Le, V.M.; Asteris, P.G. Estimation of axial load-carrying capacity of concrete-filled steel tubes using surrogate models. *Neural Comput. Appl.* **2021**, *33*, 3437–3458. [CrossRef]
34. Smys, S.; Balas, V.E.; Kamel, K.A.; Lafata, P. *Inventive Computation and Information Technologies*; Springer: Berlin/Heidelberg, Germany, 2021.
35. Samantaray, S.; Sumaan, P.; Surin, P.; Mohanta, N.R.; Sahoo, A. Prophecy of groundwater level using hybrid ANFIS-BBO approach. In *Proceedings of International Conference on Data Science and Applications: ICDSA 2021*; Springer: Berlin/Heidelberg, Germany, 2022; Volume 1, pp. 273–283.

36. Joshi, H.; Arora, S. Enhanced grey wolf optimization algorithm for global optimization. *Fundam. Informaticae* **2017**, *153*, 235–264. [CrossRef]
37. Qais, M.H.; Hasanien, H.M.; Alghuwainem, S. Augmented grey wolf optimizer for grid-connected PMSG-based wind energy conversion systems. *Appl. Soft Comput.* **2018**, *69*, 504–515. [CrossRef]
38. Gupta, S.; Deep, K.; Mirjalili, S. An efficient equilibrium optimizer with mutation strategy for numerical optimization. *Appl. Soft Comput.* **2020**, *96*, 106542. [CrossRef]
39. Ding, Q.; Xu, X. Improved GWO Algorithm for UAV Path Planning on Crop Pest Monitoring. Issue Special Issue on Multimedia Streaming and Processing in Internet of Things with Edge Intelligence. *Int. J. Interact. Multimed. Artif. Intell.* **2022**, *7*, 30–39. [CrossRef]
40. Rosenblatt, F. The perceptron: A probabilistic model for information storage and organization in the brain. *Psychol. Rev.* **1958**, *65*, 386. [CrossRef]
41. Chen, H.; Asteris, P.G.; Armaghani, D.J.; Gordan, B.; Pham, B.T. Assessing dynamic conditions of the retaining wall: Developing two hybrid intelligent models. *Appl. Sci.* **2019**, *9*, 1042. [CrossRef]
42. Armaghani, D.J.; Ming, Y.Y.; Mohammed, A.S.; Momeni, E.; Maizir, H. Effect of Different Kernels of the Support Vector Machine to Forecast the Bearing Capacity of Deep Foundation. *J. Soft Comput. Civ. Eng.* **2023**, *7*, 111–128.
43. Ahmed, H.U.; Mohammed, A.S.; Faraj, R.H.; Abdalla, A.A.; Qaidi, S.M.A.; Sor, N.H.; Mohammed, A.A. Innovative modeling techniques including MEP, ANN and FQ to forecast the compressive strength of geopolymer concrete modified with nanoparticles. *Neural Comput. Appl.* **2023**, *35*, 12453–12479. [CrossRef]
44. Asteris, P.G.; Tsaris, A.K.; Cavaleri, L.; Repapis, C.C.; Papalou, A.; Di Trapani, F.; Karypidis, D.F. Prediction of the fundamental period of infilled RC frame structures using artificial neural networks. *Comput. Intell. Neurosci.* **2016**, *2016*, 20. [CrossRef] [PubMed]
45. He, B.; Armaghani, D.J.; Lai, S.H. Assessment of tunnel blasting-induced overbreak: A novel metaheuristic-based random forest approach. *Tunn. Undergr. Space Technol.* **2023**, *133*, 104979. [CrossRef]
46. Indraratna, B.; Armaghani, D.J.; Correia, A.G.; Hunt, H.; Ngo, T. Prediction of resilient modulus of ballast under cyclic loading using machine learning techniques. *Transp. Geotech.* **2023**, *38*, 100895. [CrossRef]
47. Shan, F.; He, X.; Armaghani, D.J.; Zhang, P.; Sheng, D. Success and challenges in predicting TBM penetration rate using recurrent neural networks. *Tunn. Undergr. Space Technol.* **2022**, *130*, 104728. [CrossRef]
48. Li, D.; Liu, Z.; Xiao, P.; Zhou, J.; Armaghani, D.J. Intelligent rockburst prediction model with sample category balance using feedforward neural network and Bayesian optimization. *Undergr. Space* **2022**, *7*, 833–846. [CrossRef]
49. Paryani, S.; Neshat, A.; Javadi, S.; Pradhan, B. Comparative performance of new hybrid ANFIS models in landslide susceptibility mapping. *Nat. Hazards.* **2020**, *103*, 1961–1988. [CrossRef]
50. Mustafa, R.; Samui, P.; Kumari, S. Reliability Analysis of Gravity Retaining Wall Using Hybrid ANFIS. *Infrastructures* **2022**, *7*, 121. [CrossRef]
51. Jang, J.-S. ANFIS: Adaptive-network-based fuzzy inference system. *IEEE Trans. Syst. Man. Cybern.* **1993**, *23*, 665–685. [CrossRef]
52. Mirjalili, S.; Mirjalili, S.M.; Lewis, A. Grey Wolf Optimizer. *Adv. Eng. Softw.* **2014**, *69*, 46–61. [CrossRef]
53. Nadimi-Shahraki, M.H.; Taghian, S.; Mirjalili, S. An improved grey wolf optimizer for solving engineering problems. *Expert Syst. Appl.* **2021**, *166*, 113917. [CrossRef]
54. Tumar, I.; Hassouneh, Y.; Turabieh, H.; Thaher, T. Enhanced binary moth flame optimization as a feature selection algorithm to predict software fault prediction. *IEEE Access* **2020**, *8*, 8041–8055. [CrossRef]
55. Tiachacht, S.; Khatir, S.; Le Thanh, C.; Rao, R.V.; Mirjalili, S.; Wahab, M.A. Inverse problem for dynamic structural health monitoring based on slime mould algorithm. *Eng. Comput.* **2021**, *38*, 2205–2228. [CrossRef]
56. AlRassas, A.M.; Al-Qaness, M.A.A.; Ewees, A.A.; Ren, S.; Sun, R.; Pan, L.; Elaziz, M.A. Advance artificial time series forecasting model for oil production using neuro fuzzy-based slime mould algorithm. *J. Pet. Explor. Prod. Technol.* **2022**, *12*, 383–395. [CrossRef]
57. Al-Qaness, M.A.A.; Ewees, A.A.; Fan, H.; Abualigah, L.; Elaziz, M.A. Marine predators algorithm for forecasting confirmed cases of COVID-19 in Italy, USA. Iran and Korea. *Int. J. Environ. Res. Public Health* **2020**, *17*, 3520. [CrossRef]
58. Mirjalili, S. Moth-flame optimization algorithm: A novel nature-inspired heuristic paradigm. *Knowl. Based Syst.* **2015**, *89*, 228–249. [CrossRef]
59. Li, S.; Chen, H.; Wang, M.; Heidari, A.A.; Mirjalili, S. Slime mould algorithm: A new method for stochastic optimization. *Futur. Gener. Comput. Syst.* **2020**, *111*, 300–323. [CrossRef]
60. Faramarzi, A.; Heidarinejad, M.; Mirjalili, S.; Gandomi, A.H. Marine Predators Algorithm: A nature-inspired metaheuristic. *Expert Syst. Appl.* **2020**, *152*, 113377. [CrossRef]
61. ASTM Committee D-18 on Soil and Rock. *Standard Practice for Classification of Soils for Engineering Purposes (Unified Soil Classification System)*; ASTM International: West Conshohocken, PA, USA, 2017.
62. Taylor, K.E. Summarizing multiple aspects of model performance in a single diagram. *J. Geophys. Res. Atmos.* **2001**, *106*, 7183–7192. [CrossRef]